

*Review Article***Direction selectivity of the retinotectal system of fish: findings based on microelectrode extracellular recordings of the tectum opticum**Ilija Damjanović¹, Alexey Aliper¹, Paul Maximov¹, Alisa Zaichikova¹, Zoran Gačić^{2,*} and Elena Maximova¹¹*Institute for Information Transmission Problems, Russian Academy of Sciences, Moscow, Russia*²*University of Belgrade, Institute for Multidisciplinary Research, Belgrade, Serbia****Corresponding author:** zorga@imsi.rs**Received:** December 16, 2023; **Revised:** January 3, 2023; **Accepted:** January 5, 2023; **Published online:** January 20, 2023

Abstract: Vision in fish plays an important role in different forms of visually guided behavior. The visual system of fish is available for research by different methods; it is a convenient experimental model for studying and understanding the mechanisms of vision in general. Responses of retinal direction-selective (DS) ganglion cells (GCs) are recorded extracellularly from their axon terminals in the superficial layers of the tectum opticum (TO). They can be divided into three distinct groups according to the preferred directions of stimulus movement: caudorostral, dorsoventral and ventrodorsal. Each of these groups comprises both ON and OFF units in equal proportions. Relatively small receptive fields (3–8°) and fine spatial resolution characterize retinal DS units as local motion detectors. Conversely, the responses of direction-selective tectal neurons (DS TNs) are recorded at two different tectal levels, deeper than the zone of retinal DS afferents. They are characterized by large receptive fields (up to 60°) and are indifferent to any sign of contrast, i.e., they can be considered as ON-OFF-type units. Four types of ON-OFF DS TNs preferring different directions of motion have been recorded. The preferred directions of three types of DS TNs match the preferred directions of three types of DS GCs. Matching the three preferred directions of ON and OFF DS GCs and ON-OFF DS TNs has allowed us to hypothesize that the GCs with caudorostral, ventrodorsal and dorsoventral preferences are input neurons for the corresponding types of DS TNs. On the other hand, the rostrocaudal preference in the fourth type of DS TNs, recorded exclusively in the deep tectal zone, is an emergent property of the TO. In this review, our findings are compared with the results of other authors examining direction selectivity in the fish retinotectal system.

Keywords: tectum opticum; motion detectors; retinal direction-selective; direction-selective ganglion cells; direction-selective tectal neurons

INTRODUCTION

Vision in fish plays an important role in different forms of visually guided behavior, including object detection and recognition, orientation and navigation, foraging and avoiding predators, etc. A significant part of visual processing occurs within the retina of the eye. Ganglion cells (GCs) are the final output neurons in retinal information processing. An entire visual scene is encoded by many different types of GCs whose receptive fields (RFs) are distributed over the image plane at the retinal surface. The information processed by the specialized GCs (“retinal detectors”) is transmitted to the primary

visual centers of the fish brain, mainly the midbrain formation tectum opticum (TO) [1-4].

The physiological properties of different types of retinal detectors can be successfully studied by extracellular recording of the single-unit responses of GCs from their axon terminals at different depths of the TO. This method was first developed for the study of frog retinotectal projections, and described in the classic work “What the frog’s eye tells the frog’s brain?” [5-6]. Experiments were performed on intact animals. Single unit responses of the motion detectors were recorded extracellularly from their axon terminals in

the superficial layers of the midbrain formation TO using low impedance (200-500 K Ω) microelectrodes prepared according to the published procedure [7]. The electrodes were made using micropipettes filled with Wood's metal and tipped with a platinum cap 2-10 μm in diameter. It was shown that the afferents of different types of local edge detectors (LEDs) terminate at different depths of the frog TO.

The method of Lettvin et al. was later used in visual information processing research in the retinotectal systems of various fish species [8-15]. These early electrophysiological studies performed on immobilized intact fish revealed the laminar organization of retinal afferents in the fish TO. In experiments from our group, it was shown that axon terminals of different types of retinal GCs are clustered at different depths of the tectal retinorecipient area [11,15]. In the superficial sublayers, responses of direction-selective (DS) units were constantly recorded. Another cluster of retinal units was recorded in the deeper sub-lamina. The first type of units in this cluster is not direction selective and responds to small contrasting spots moving in various directions. These units resemble LEDs of the frog retinotectal system [5]. Another two types that were recorded in the same sublayer are orientation selective (OS) GCs which are sensitive to either vertically or horizontally oriented edges. Both types of OS units are ON-OFF-type cells. Color-opponent elements were usually detected slightly deeper than the LEDs and OS GCs. Finally, in the deepest sublamina of the retinorecipient layer, the responses of the sustained units were recorded. These GCs, referred to as ON-sustained and OFF-sustained units, responded by sustained discharges to the diffuse ON and OFF flashes, respectively.

In the early studies mentioned above [11,14-15], clusters of DS GCs were not defined precisely because of technical constraints. Stimuli were presented manually and no automatic processing of the recordings from the tectum was made. Therefore, the authors managed to accurately identify only one type of retinal DS detector, which preferred a caudorostral direction of motion. In later studies, there was a need to create a complex setup that

would ensure the automatic presentation of stimuli of different characteristics and provide automatic processing of the responses of various tectal units.

A hardware-software setup for electrophysiological studies of the fish visual system

To ensure a more accurate evaluation of the properties of different types of fish retinal detectors, the experimental setup providing online data acquisition and processing was developed based on the experience from our laboratory obtained in previous decades [16] (Fig. 1). Three mutually connected and synchronized computer modules are used during the experimental work: (1) is the recording module, connected to the microelectrode through the A/D and the preamplifier; it serves for the recording of the neuron responses, further visualization of the responses on the screen and, finally, storing of the experimental data; (2) is the stimulating module that controls the stimulating CRT monitor on which various visual stimuli are presented to the fish; (3) is the controlling module, which provides efficient manipulation of stimulation and recording parameters during the experiment and additional online graphic demonstration of the processed data (on a separate monitor).

As of 2003, in a series of studies, we systematically investigated the properties of more than three

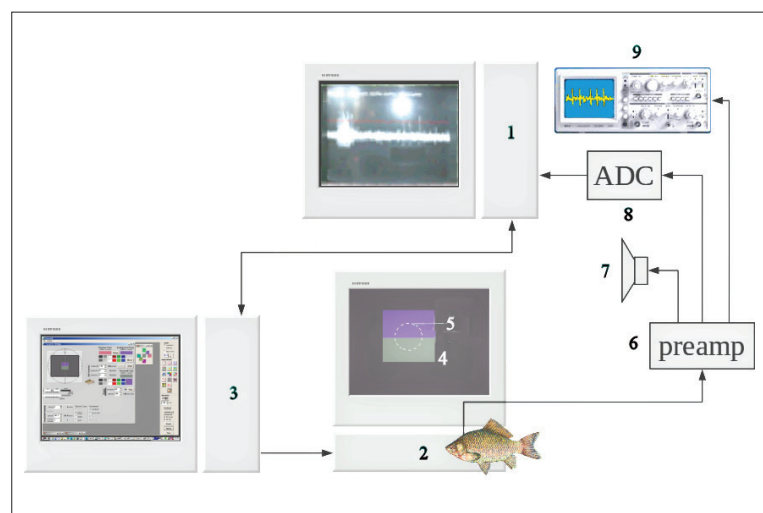


Fig. 1. Scheme of the experimental setup: 1 – recording module; 2 – stimulating module; 3 – controlling module; 4 – stimulation area on the monitor screen; 5 – receptive field of the recorded cell; 6 – AC preamplifier; 7 – loudspeaker; 8 – A/D converter; 9 – oscilloscope. Redesigned from [16].

thousand retinal detectors in the TO of different cyprinid fishes, *Carassius gibelio* (wild form of goldfish), carp, roach and a barbell fish, *Labeobarbus intermedius*. The experiments were conducted as follows: an immobilized fish (d-tubocurarine, intramuscular (i.m.) injection) was placed in its natural position in a transparent Plexiglas tank where artificial respiration was provided continuously by forcing aerated water through the gills. Visual stimuli (contrast edges, stripes and spots moving at variable speeds in different directions) were presented to the right eye of the fish on the CRT monitor screen from a distance of about 30 cm. From this distance, the screen covers $43 \times 32^\circ$ of the fish's visual field. Since preliminary findings showed that the fish DS GCs are characterized by relatively small receptive fields (RFs) of about 5° [1,16], stimuli were presented on the screen within a limited gray square-shaped area of stimulation with angular dimensions of $11 \times 11^\circ$. The stimulation area could be placed at arbitrary locations on the screen and was usually placed so that the RF of the recorded unit was located approximately in its center. We worked mainly in the lateral visual field of the right eye (the size of the visual field was $60 \times 40^\circ$). The background in the stimulation area usually had an effective radiance of $14.5 \text{ mW m}^{-2} \text{ sr}^{-1}$, while the effective radiances of the light and dark stimuli were respectively 65 and $0.13 \text{ mW m}^{-2} \text{ sr}^{-1}$. Constant brightness was maintained for the rest of the monitor screen outside of the stimulation area, with the effective radiance usually equal to $7.0 \text{ mW m}^{-2} \text{ sr}^{-1}$. The responses of different types of GCs were recorded extracellularly from their axon terminals in the retinorecipient layer of the tectum (depth of recording 50-200 μm). The low impedance microelectrode [7] was visually guided under a microscope (SZ51, Olympus, Shinjuku, Tokyo, Japan) to the TO surface and then perpendicularly advanced through the superficial tectal layers by a micromanipulator (MP-225, Sutter Instrument, Novato, CA, USA) until a stable single-unit response was recorded, which could last from a few minutes to an hour or more. Single-unit responses were gained in an AC preamplifier (band pass 100 Hz to 3.5 kHz), and listened to on a loudspeaker, monitored on an oscilloscope and digitized by an A/D converter (at 25 kHz sampling rate). The digitized data were subsequently subjected to online processing performed on a controlling computer module. The standard experimental

procedures used for data processing (polar diagrams, random checkerboard, contrast sensitivity, etc.) are designed in the form of program tools. Some of them will be described in the next chapters.

Direction-selective ganglion cells in fish: response pattern and classification of units according to their preferred directions

The classification of DS GC records by preferred direction was performed on the basis of their polar diagrams (PDs). The polar response pattern of the unit was always measured with contrast "edge" stimuli consecutively moving in 12 different directions over the gray background ("edge" stimulus, wide stripe exceeding stimulation area). The values of the stimulation parameters are specified as follows: the movement speed of the edge, the brightness of the background and the stimulus, the brightness surrounding the outside of the stimulation area, the initial direction of movement, the number of repetitive trials in each of 12 directions (usually 3). Mean spikes evoked by leading and trailing edges of stimuli were calculated over repeated trials for each direction. At the end of the procedure, a measurement for the first direction was repeated to verify the unit response level. The preferred directions of the stimulus movement were determined according to the phase of the first harmonic of the Fourier transform of the polar diagram. The mean number of spikes in the response (N) as a function of direction (φ) is approximated by a second-order harmonic function:

$$N(\varphi) = a_0 + a_1 \cdot \cos(\varphi - \varphi_1) + a_2 \cdot \cos(2\varphi - 2\varphi_2) \quad (1)$$

The amplitudes of the zero (a_0), first (a_1) and second (a_2) harmonics, and the phases of the first (φ_1) and second (φ_2) harmonics characterize the polar response patterns. In several studies, we have clearly shown that according to their polar plot patterns, GCs projecting to the tectum constitute three clear clusters: (i) those with small relative amplitudes of both first and second harmonics – nonselective units (spot detectors, color-opponent units, sustained units); (ii) those with pronounced relative amplitude of the first harmonic – direction-selective units; (iii) those with a pronounced relative amplitude of the second harmonic – orientation-selective units [1,16]. The scatter diagram of the amplitude of the second harmonic

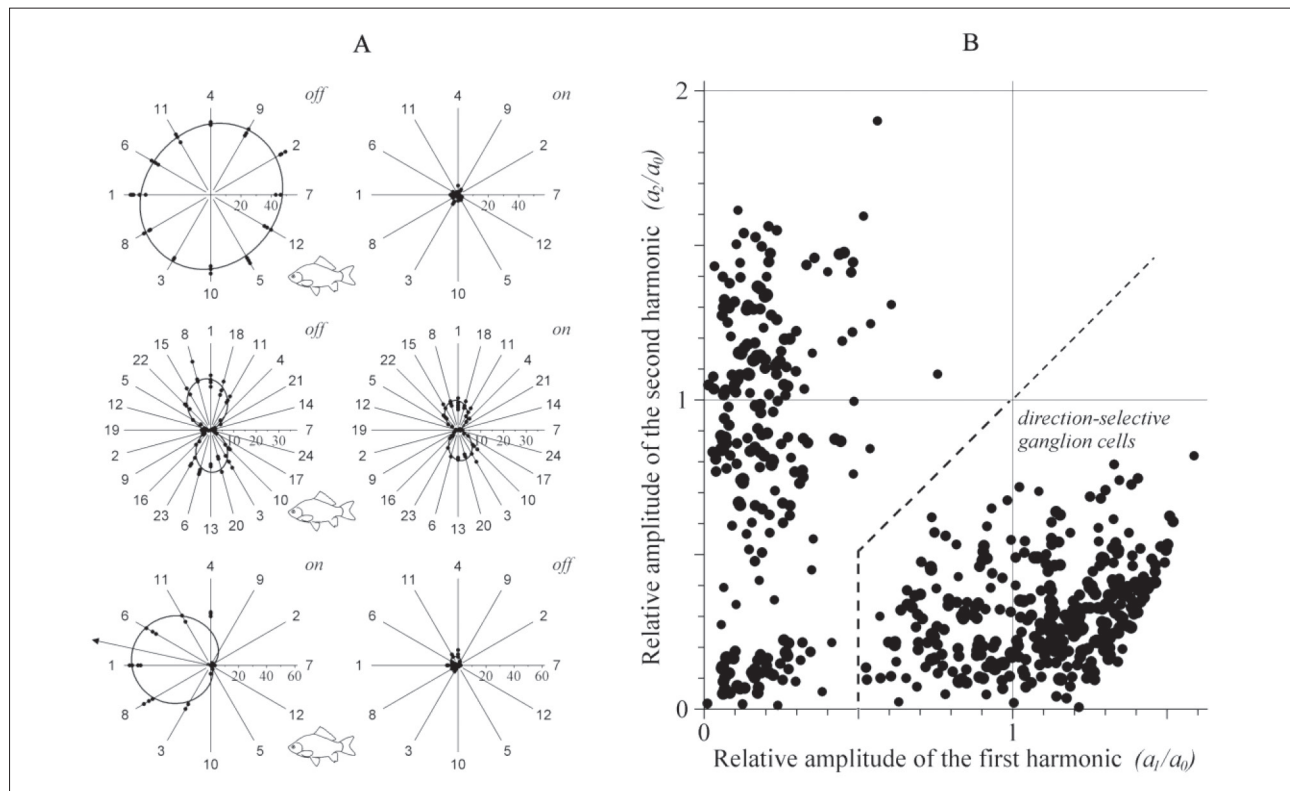


Fig. 2. Examples of three principal types of polar response patterns observed in goldfish retinal motion detectors. **A** – Polar plot of a direction selective ganglion cell as compared with polar plots of a spot detector and an orientation selective unit. The stimuli (contrast edges) moved in 12 or 24 directions at a speed of $11^\circ/\text{s}$ inside the gray stimulation area (a square with a side of approximately 11° on the monitor screen). Polar plots of responses to the leading (left panel) and trailing (right panel) edges of stimuli are shown. Dots mark the number of spikes evoked in response to each of three runs for each applied direction; solid curves represent the approximations of the experimental data by a Fourier series with first two harmonics (function (1)). The numbers on the radial lines represent the order of movement directions. The plots marked with the label “off” are built for the responses to the movement of dark edges into the receptive field (RF); those marked with label “on” are built for the responses to the movement of light edges. Orientation of the fish relative to the directions of the stimulus movement is demonstrated. Top panels: black spot detector (OFF-type unit); stimulus – black edge. Middle panels: orientation selective unit (“detector of horizontal line”; ON-OFF type unit); stimulus – black edge. Bottom panels: ON-type direction selective unit which prefers the caudorostral motion direction; stimulus – white edge; preferred direction of the stimulus movement for the unit is shown by the black arrow. “Edge” stimulus – wide stripe exceeding the stimulation area in width. **B** – Scatter diagram of the amplitude of the second harmonic (a_2) versus the amplitude of the first one (a_1) for 522 polar patterns, measured for the GCs of various types (cluster of DS units is marked). Redesigned from [16].

(a_2) versus the amplitude of the first harmonic (a_1) for 522 polar patterns, measured for GCs of various types, is presented in Fig. 2B, with the cluster of DS units marked.

The two PDs shown in Fig. 2A (bottom panels) represent the responses of a goldfish ON-type DS unit to the leading and trailing edges of the white stimuli; this particular GC preferred the caudorostral motion direction. The leading edges of the stimuli evoked considerable excitation of the unit when the motion direction was close to the preferable one. PD is approximated by function (1); the preferred direction is

marked by an arrow. However, the same DS unit did not respond to the trailing edges of the same stimuli, regardless of their direction of movement, i.e. it remained silent to the RF darkening. Two other types of retinal detector PDs projected to the tectum, with a spot detector and an OS unit given for comparison in Fig. 2A (top and middle panels, respectively).

The typical response pattern of a roach DS GC evoked by an “edge” stimulus moving in the preferred direction is presented in Fig. 3B. This DS GC responded only to the introduction of the white stimulus into the RF and can be considered as an ON-type DS unit.

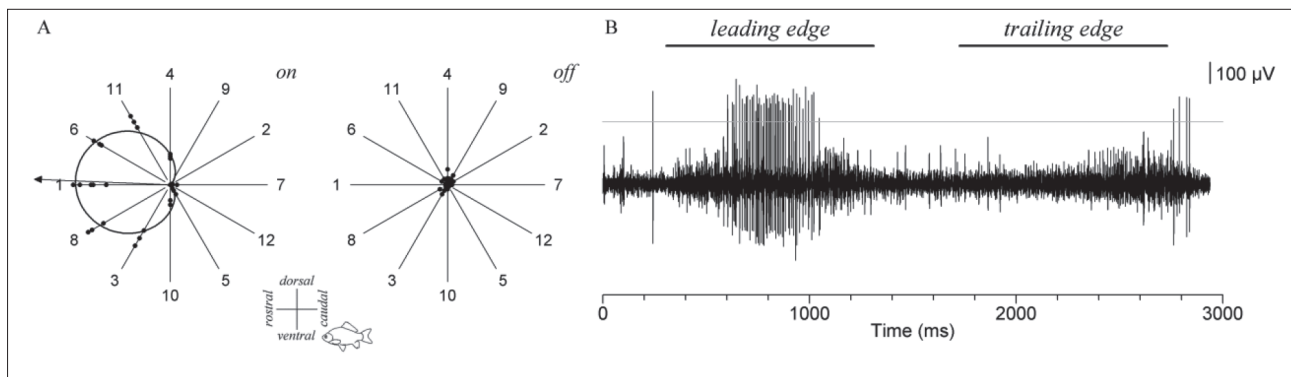


Fig. 3. The response of a roach ON DS unit of retinal origin with a caudorostral preference. **A** – PDs of a roach ON DS GC to the leading and trailing edges of white broad stripes (light “edge” stimuli). All conventions are same as in Fig. 2A. **B** – Response of the same unit to the leading and trailing edges of the white stimulus moving in the preferred, caudorostral direction. To select a single unit response, we used amplitude discrimination (horizontal thin line). Only spikes exceeding the amplitude criterion were used for further analysis (e.g. for the measurement of PDs). Redesigned from [48].

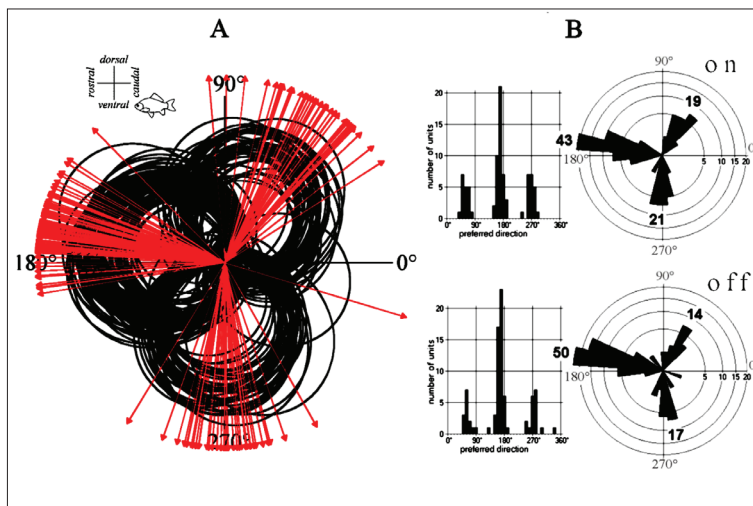


Fig. 4. Preferred directions of goldfish DS GCs. **A** – Clustering of polar response patterns calculated for 164 goldfish DS GCs (preferred directions calculated for directional tuning curves are marked by red arrows). **B** – ON- and OFF-type DS GCs were presented in practically equal quantities in the tested units. Histograms of preferred directions for both types of DS units are presented. The orientation of the fish relative to the directions of stimulus movement is demonstrated. Redesigned from [1].

The short duration of the spike discharge evoked by the leading edge of the stimulus indicated a relatively small RF, which is characteristic for DS units of retinal origin. Note that the PDs measured for the DS GC of the roach (Fig. 3A) are shaped almost the same as those shown in Fig. 2A for goldfish DS GC.

Detailed analysis of measured PDs on the new setup revealed six distinct types of DS GCs projecting to the fish tectum. According to their preferred direction, DS GCs comprise three distinct groups

(caudorostral, ventrodorsal and dorso-ventral), with each group containing DS GCs of ON and OFF subtypes approximately in equal quantity [1,16]. It was surprising that fish DS GCs projecting to the TO according to their preferred directions substantially differed from mammalian retinal DS units projecting to the superior colliculus; a variety of rabbit and mouse DS GCs was comprised of four types of ON-OFF cells with the preferred directions separated by about 90° [17-21]. This difference between fish and mammalian DS units will be discussed later. All polar plots measured in goldfish DS GCs before the year 2005 are shown in Fig.4A. The preferred directions calculated by the phase of the first harmonic of the Fourier transform are marked by arrows. ON- and OFF-type DS GCs were presented in equal quantities among the

tested units (Fig. 4B). Units that responded to the caudorostral direction of stimulus movement were the most numerous. Based on subjective judgment (from our experience accumulated during many years of research on the subject), the caudorostral DS responses of the retinal origin were recorded in TO more superficially than the responses of the dorso-ventral and ventrodorsal DS units. The results of our recent experiments performed in carp, roach and barbell fish (*Labeobarbus intermedius*) indicated that the DS GCs of these fish are equal to the retinal DS units

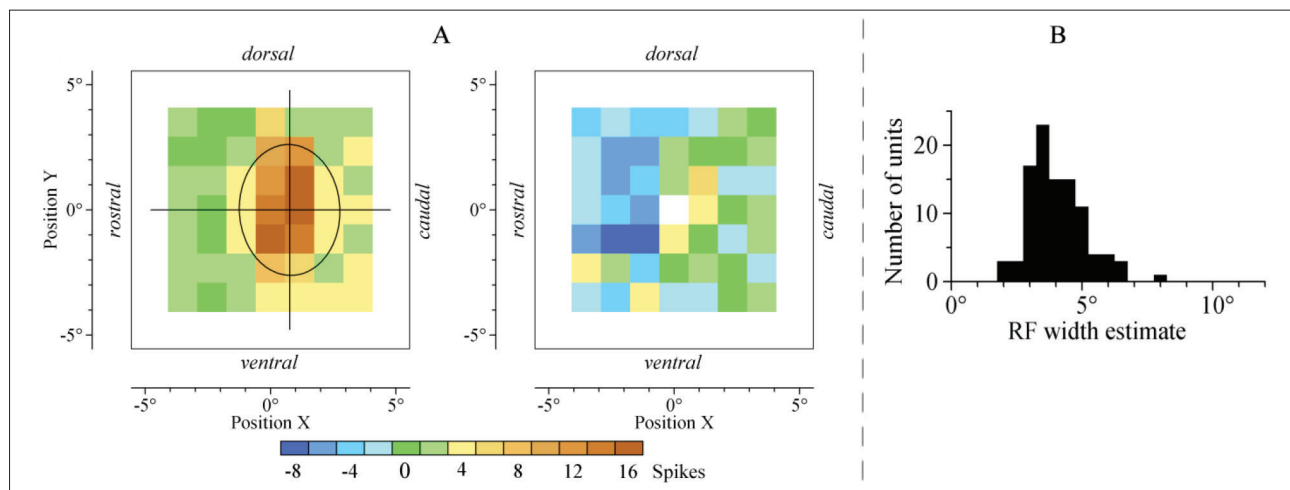


Fig. 5. Receptive field mapping of one goldfish OFF DS ganglion cell preferring the caudorostral direction of stimulus movement (random checkerboard method). **A** – Left panel: cell responsiveness across the stimulation area, recorded by RF mapping with one flashing black spot against a light background. Flashing spots were presented six times at each position. The number of spikes was counted after each turn. Cell responses over the entire stimulation area measured by this method are represented in the form of a topographic map (see the scale at the bottom of Fig. 5A). The major and minor axes of the RF were evaluated according to the two-dimensional equivalent of the standard deviation for this data set. The ellipse built based on the evaluated RF axes, presents an estimate of the RF area. Right panel: lateral interactions in the RF of the same OFF caudorostral DS unit measured by two flashing spots. The influence of the second spot (located at a different position in the stimulation area) on the response of the central one was determined by the difference between the mean number of spikes in response to simultaneous stimulation of the two spots and the mean number of spikes in response to the central stimulus alone. The differences were mapped considering the position of the second spot. **B** – Distribution of the RF sizes evaluated by a random checkerboard for 99 DS GCs (mean value $4.3 \pm 1.1^\circ$). Redesigned from [23].

of *C. gibelio* [22]. At present, our database contains 1912 PD files for various retinal DS units. This data does not differ significantly from that presented in Fig. 4. Our findings have been confirmed in another study [2]. Visually evoked activity of the retinal GC axons innervating the tectum of zebrafish larvae was recorded using calcium imaging techniques. Three subtypes of retinal DS units projecting to zebrafish tectum, characterized by preferred directions similar to those described in *C. gibelio*, were identified. The proportion of DS GC subtypes was practically the same as shown in *C. gibelio* (units with a preference for the caudorostral direction were the most numerous). It was also revealed that the projections of caudorostral units were located dorsally relative to the ventrodorsal and dorsoventral ones. The authors have not been able to classify zebrafish retinal DS units by their selectivity to ON, OFF, or ON-OFF because of the method constraints. However, similar results to those obtained in our experiments and the study of Nikolaou et al. [2] indicate that the system of DS GCs comprising six physiologically distinct subtypes might be a universal retinal DS circuit in teleost fish.

Mapping of the ganglion cell receptive field by the random checkerboard method

Receptive field sizes corresponding to six types of DS GCs were evaluated on the basis of four different methods developed in the framework of our experimental setup [23]. RFs of *Carassius gibelio* DS GCs were mapped using contrast moving stimuli (edges and spots), and additionally by the random checkerboard method using a stationary flashing spot as the stimulus. The result of the random checkerboard test on one OFF DS unit is shown in Fig. 5A (left panel). The area of stimulation was divided into 49 small squares (spots) slightly wider than 1° in size. At the beginning of the procedure, a flashing spot was presented in the central position. After that, the spot flashes were presented sequentially in nodes of a square grid in a quasi-random order. At the end of the procedure, stimulation was repeated at the central position to verify the unit response level. Cell responses to flashing spots over the entire stimulation area that were measured by this method are represented in the form of a topographic map (see the scale at the bottom

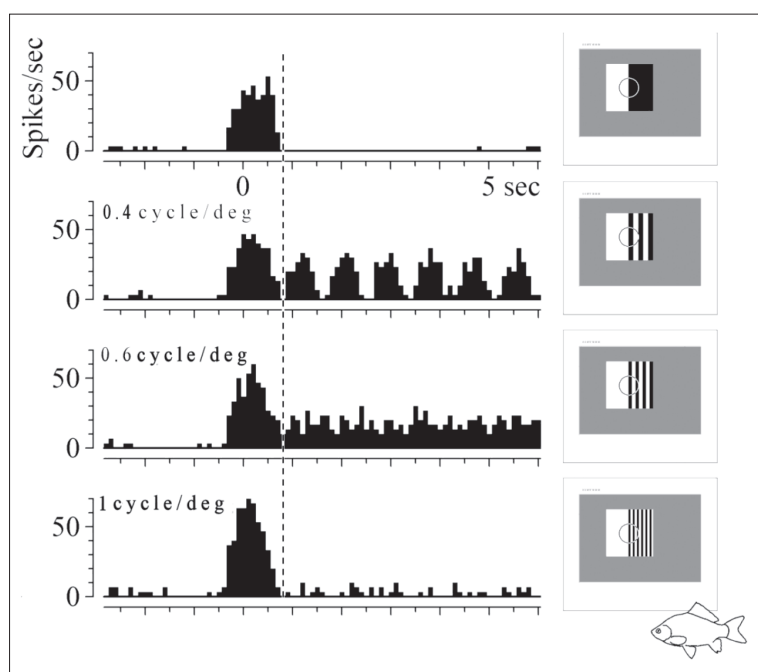


Fig. 6. Spatial properties of a goldfish OFF DS GC that prefers the caudorostral direction of stimulus movement. A schematic view of the experimental paradigm. Naturalistic images of displays on the right are given to make it possible to compare the RF size of the cell and the grating periods. The stimulation began with the presentation of the moving “edge”, i.e. a wide stripe exceeding the stimulation area (see the stimulus on the top). Subsequently, square-wave gratings of various spatial frequencies moving at a certain speed ($2.5^\circ/\text{sec}$) in a preferential direction (caudorostral in the present case) were presented to fish in the square stimulation area. The rounded area in the square represents the unit receptive field. Peristimulus histograms of the recorded responses are presented near the corresponding stimuli. The first discharge evoked by the leading edge of the grating was discarded and the remaining response was analyzed (the starting point for data processing is marked by a vertical dashed line). Note that the shown DS unit finally ceased to respond to grating of high spatial frequency (1 cycle/degree), and only a burst to the leading edge of the grating remains. A detailed explanation is given in the text. Redesigned from [24].

of Fig. 5A). The extension (length and width) and orientation of the RF were evaluated according to the two-dimensional equivalent of the standard deviation for this data set. Based on the estimated extension of the two principal axes of the RF, an ellipse was constructed. Such an ellipse was an estimate of the RF area, its diameter evaluated as a geometric mean of its length and width. A histogram of RF size distribution, estimated for 99 DS units and evaluated by this method, is presented in Fig. 5B. RF sizes, estimated on the geometric mean of the length of the major and minor axes of an ellipse, varied from 1.8° to 7° , with a mean value of $4.3 \pm 1.1^\circ$ (Fig. 5B). RF size of DS GC estimated by a random checkerboard coincided with

RF sizes measured with moving edges and spots; the mean values of the RF obtained in all applied procedures ranged between 4° and 4.8° [22]. The consistent size of the DS GCs’ receptive fields was evaluated with moving stimuli in our previous studies [1,11,16]. The right panel in Fig.5A represents the method with two simultaneous flashing spots used to analyze lateral interactions in the RF of the DS units.

Spatial resolution of direction-selective ganglion cells

We used a separate experimental procedure to measure the spatial resolution of DS GCs in goldfish and carp [24]. Spike activity of DS GCs was recorded in response to the movement of square-wave gratings of various spatial frequencies into the RF and by flowing them through it at a certain speed in a preferred direction. The other stimulation parameters (the speed of movement, the brightness of the background and of the grating, as well as the brightness of the surroundings outside the stimulation area and the number of repeated runs of each grating) were specified in advance. The measurement began with the presentation of the moving “edge” stimulus. Then, a series of gratings of increasing spatial frequency were presented automatically. The finest grating used had a frequency of 1.8 cycles per degree. At the end of the procedure, the initial moving edge stimulus was repeated. As shown in Fig.6, during data analysis we discarded the initial pulse of the unit response to the movement of the leading edge of the grating, and the remaining response was processed. The minimum resolvable angle for the tested unit was determined as the period of the first indistinguishable grating.

A rough estimate based on morphological data has shown that the fish retinal DS units receive inputs from more than 200 cones [23,25-26]. If the inputs from photoreceptors transmitted through bipolar cells were linearly summed, this would worsen the spatial

resolution of the DS GCs. However, it was proven that fish DS GCs are nonlinear integrators [24]. The results of the experiment on one goldfish DS GC are demonstrated in Fig.6. Peristimulus histograms of unit responses to different gratings are shown. The histogram on the top represents the cell's response to the movement of the black "edge" into the RF of the cell. According to the width of the evoked discharge, the RF size of the cell was determined at 4.5° . Three peristimulus time histograms of the responses to the moving gratings of increasing frequency are shown below. At first, the cell responds by separate discharges to each stripe of the drifting grating with a spatial frequency of 0.4 cycle/deg. Then, after the spatial frequency of the stimulus was increased, the response discharges merged into a continuous discharge with a spatial frequency of 0.6 cycle/deg. In other words, at this spatial frequency, the cell loses its ability to resolve stripes, but is still capable of detecting the grating. Finally, at the spatial frequency of 1 cycle/degree, the DS unit ceased to respond to the stimulus. Obviously, the minimum resolvable angle measured for the tested DS GC was considerably lower than that determined by the size of the unit RF. Similar results were obtained for all 73 DS units tested. If DS GCs were linear integrators, then their spatial resolution would be determined by the sizes of their receptive fields, which are about 4.5° . However, their minimum resolvable angle amounted to only $42'$, being approximately two-fold higher than the theoretical limit defined by the cone density [24]. In other words, it was shown that goldfish retinal DS units, like other movement detectors, are nonlinear integrators, with the visual acuity close to the limit determined by the density of the cones.

Contrast sensitivity of direction-selective ganglion cells

Besides the extremely high spatial resolution, goldfish DS GCs are characterized by remarkable contrast sensitivity. For systematic, precise measurements of DS GC contrast sensitivity, we developed a specific experimental procedure [16]. Wide contrast stripes of different brightness exceeding the receptive field of the studied DS unit were moved in a preferred direction across a neutral gray background, and the number of spikes evoked by the leading and trailing edges of the stimuli was counted. Based on the recorded responses

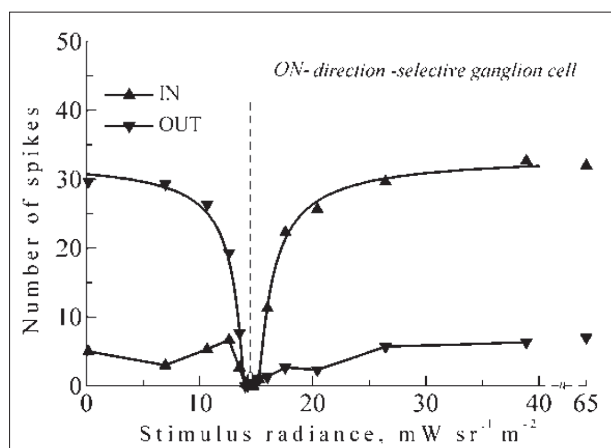


Fig. 7. Contrast sensitivity of goldfish DS GCs. Intensity-response profiles showing the responses of one goldfish ON-type DS GC as a function of the light intensity ("stimulus radiance"). The ordinate indicates the number of spikes (mean of three runs) in the cell discharge in response to the movement of achromatic wide stripes of various brightness over a fixed gray background through the receptive field in a preferential direction. Two branches of the curve correspond to responses to the leading (in) and trailing (out) edges of the stimulus. The presented DS GC was selective to caudo-rostral movement, stimulated by vertical edges moving in the caudo-rostral direction. The background radiance was equal to $14.5 \text{ mWsr}^{-1} \text{ m}^{-2}$ (marked with a dashed line), and the speed of the stimuli was $11^\circ/\text{s}$. Redesigned from [16].

the graphs were constructed, representing the dependence of the mean number of spikes on the brightness of stimuli (Fig. 7; note the data for an ON DS unit). On the graphs, amplitudes of responses evoked by the leading ("IN") and trailing edges ("OUT") of the applied stimuli are presented separately. The "IN" and "OUT" intensity-response profiles were separately approximated by the two-parameter hyperboles (steep profiles in Fig. 7). The crossing points of the hyperboles with the abscissa define the increment and decrement threshold values. More than 100 DS units were studied. Recorded threshold contrasts for all data varied between 1.1% and 6.4%, with a mean value of about 3% of background brightness [16]. The saturation of profiles at low contrast stimuli indicated that the responses of the retinal DS units were practically independent of the stimulus intensity in all the DS GCs studied.

The properties of fish retinal DS GCs projecting to the tectum and the relatively small RF sizes were characterized by a fine spatial resolution as local motion detectors. This assumption is supported by the

fact that the fish DS units respond to a broad range of velocities of moving stimuli (from 2-30°/sec) [16]. Since DS GCs are characterized by remarkable contrast sensitivity, they are most likely involved in the detection and tracking of small contrasting objects moving in the surrounding environment. According to their physiological properties, fish DS GCs resemble the fast DS GCs of the mammalian retina projecting to the superior colliculus [17-19]. These DS units, specified as local motion detectors, are also characterized by fine spatial resolution and are independent of velocity [27-29]. However, it is important to note that our experiments revealed some essential differences between fish and mammalian fast DS GCs. According to their preferred directions, fish DS GCs were assumed to be comprised of three distinct groups, each of them containing units of ON and OFF subtypes in approximately equal ratios, while the mammalian DS GCs are represented by four types of ON-OFF cells with the preferred directions separated by about 90° [20-21].

The fine structure of the fish direction-selective ganglion cells' receptive field

The basic requirement for direction selectivity is an asymmetric nonlinear interaction between spatially separate inputs [17]. In theory built for rabbit DS GCs, this asymmetry could arise from increased inhibition during null direction motion or from increased excitation when the stimulus moves in the preferred direction. Thus, in a simplified excitatory model, the input at each position is facilitated by the prior inputs coming from the preferred side of the cell RF. In a simplified inhibitory model, the excitatory input at each position is blocked by prior inputs coming from the null side. The main data on the mechanism of direction selectivity were obtained in mammals (mainly rabbit and mouse retinas). The crucial role of the null-side inhibition in the generation of direction selectivity in the retina was proved for mammalian DS GCs. It was demonstrated that asymmetric null-side inhibition is largely mediated by direction-selective dendrites of starburst amacrine cells (SACs) [21,30]. The underlying mechanism of direction selectivity in fish retina was investigated less thoroughly. Since starburst-like amacrine cells were described in morphological studies on shark [31] and zebrafish [32-33], it can be assumed that inhibition from the null side of

the DS GC receptive field induces direction selectivity in the fish retina similar to mammalian DS GCs.

We used two different procedures to analyze the lateral interactions in the RF of the fish retinal DS units. In the first one, the stimulation area was divided into small squares in the same way as in the random checkerboard method. At the beginning of the procedure, the central flashing spot was presented as a reference stimulus. After that, two spots flashed simultaneously, one of them always in the center and the second in different positions of the stimulation area in a quasi-random order. Both spots flashed simultaneously in each position, and the number of evoked spikes was counted. At the end of the procedure, stimulation was repeated at the central position to verify the unit response level. The influence of the second spot on the response to the central one was determined by the difference between the number of spikes in response to the stimulation of the two spots and the number of spikes in response to the reference stimulus alone. When this value was negative, one could say that there was an inhibitory influence of the second spot. These differences were mapped considering the position of the second flickering spot. Fig. 5A (right panel) illustrates the results obtained for an OFF caudorostral unit (its RF is mapped on the left panel of Fig. 5A). An inhibitory (blue) area is adjacent to the side of the RF pointing in the null direction (RF null side). Similar results were obtained for the other 15 DS units [23]. Accordingly, this confirms that the null-side inhibition underlies the mechanism of direction selectivity in the fish retina.

Hence, the method with two-spot stimulation proved to be relevant for the analysis of lateral interactions between the peripheral inhibitory zone and the RF center. However, the spread of null-side inhibitory influences across the RF could not be adequately studied by this method. To more accurately estimate the spatial properties of null-side inhibition in the RF of fish retinal DS units, another experimental procedure was developed [22]. DS GCs were stimulated by pairs of narrow stripes moving in opposing directions towards each other in the RF. One stripe entered the RF from the preferred side, and the other one from the null side (Fig. 8A). The method with paired moving stripes can be used for reliable estimation of the distance between approaching stimuli at which the inhibitory signal sent from the RF null side starts to

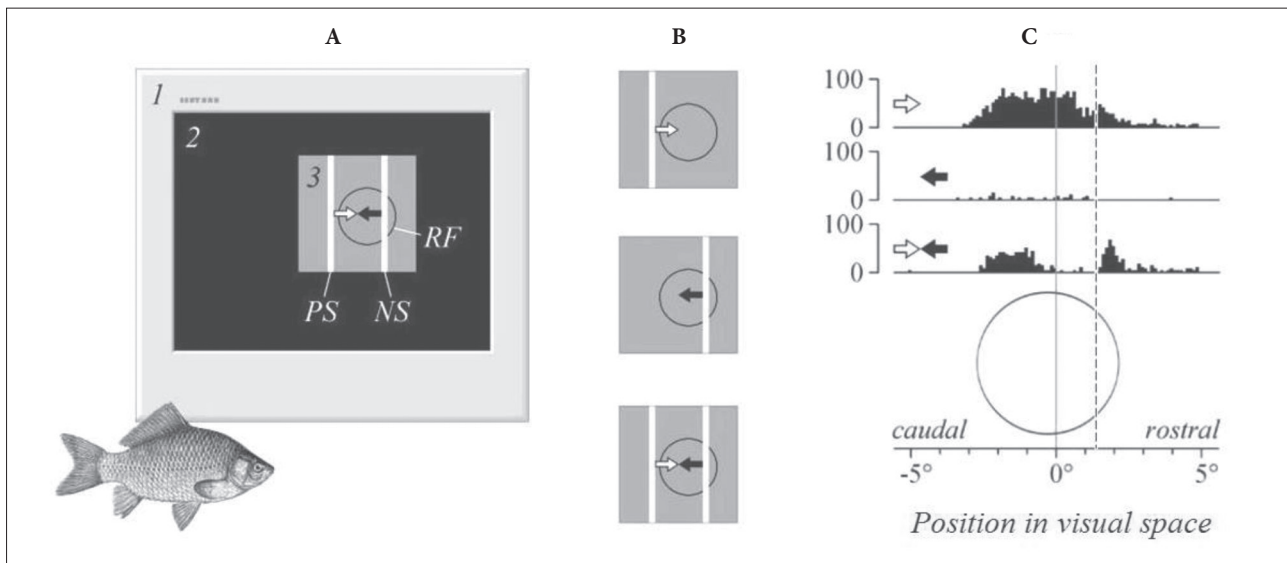


Fig. 8. Stimulation procedure with paired stripes moving in opposing directions. A – A schematic presentation of the experimental paradigm. 1 – stimulating monitor; 2 – monitor screen; 3 – gray stimulation area (angular dimensions of $11 \times 11^\circ$); RF – rough estimation of the receptive field of the recorded unit with regard to the stimulation area; PS – preferred-side stripe; NS – null-side stripe. Paired stripes (PS and NS) move simultaneously in opposing directions – one stripe enters the cell RF from the preferred direction and the other one from the null direction (marked by a white and black arrow, respectively). B – An example of the experimental procedure performed on a goldfish ON-type caudorostral DS GC. The unit was stimulated by white stripes, moving in either preferred or null directions across the gray stimulation area. Stimulation areas are schematically presented by gray square-shaped regions. Modes of stimulation: top panel – single stripe moving in the preferred direction; middle panel – single stripe moving in the null direction; bottom panel – paired stripes moving simultaneously in opposing directions (paired stimuli cross in the middle of the stimulation area and afterwards move away from each other). The width of stimuli was $30'$; the velocity of stimulus movements was $5.5^\circ/s$. The rounded area in the square represents the approximation of the unit RF. C – Eighteen consecutive presentations of stimuli were performed at each step of stimulation. Averaged peristimulus histograms of unit-evoked responses, calculated for all 3 modes of stimulation are presented in the same order as in B. Spatial coordinates of the stimulation area are presented at the bottom of the diagram in the coordinates of visual space (degrees; 0° marks the center of the stimulation area). The rounded area represents a rough estimation of the unit RF. The inhibitory effect mediated from the null direction lasted during the approach of stimuli – the response evoked by the preferred-side stripe was completely suppressed. After the stripes crossed each other in the center of the stimulation area the response of the unit regenerated. Dashed vertical line marks the position of the preferred stripe (PS) when the unit response to paired stimuli started to recover. Redesigned from [22].

influence the response elicited by the movement of the stimulus in the preferred direction. The experimental procedure is as follows: in the first two steps of stimulation, the single stripe moves in the preferred and null directions (top and middle panel of Fig. 8B); in the third step of the procedure, the DS units are stimulated by paired stripes that move simultaneously in opposing directions, one of them moving across the stimulation area in the preferred, and the other one in the null direction (bottom panel of Fig. 8B). The stimuli merge at the center of the stimulation area and subsequently move away from each other. In different experiments, stimulation was repeated either 9 or 18 times for each kind of stimulus. Averaged peristimulus time histograms of the responses of one ON DS unit of *C. gibelio* calculated for three modes of stimulation are shown in Fig. 8C. The cell response, evoked by the

stripe coming from the preferred side of the RF was inhibited by the stimulus coming from the opposite direction. The inhibitory effect mediated from the null direction was recorded while the stimuli were approaching, and it ceased after the stripes crossed each other in the center of the stimulation area.

The processed data were subjected to further statistical analysis to precisely establish the beginning of inhibition. The peristimulus time histograms calculated for paired stripes were compared with those calculated for stimulation with the preferred stimulus alone. The aim of the procedure was to estimate the position of the preferred stimulus in the RF at which the inhibitory signal was initiated. For this purpose, the numbers of spikes elicited by the single preferred stripe and paired opposing stimuli were compared

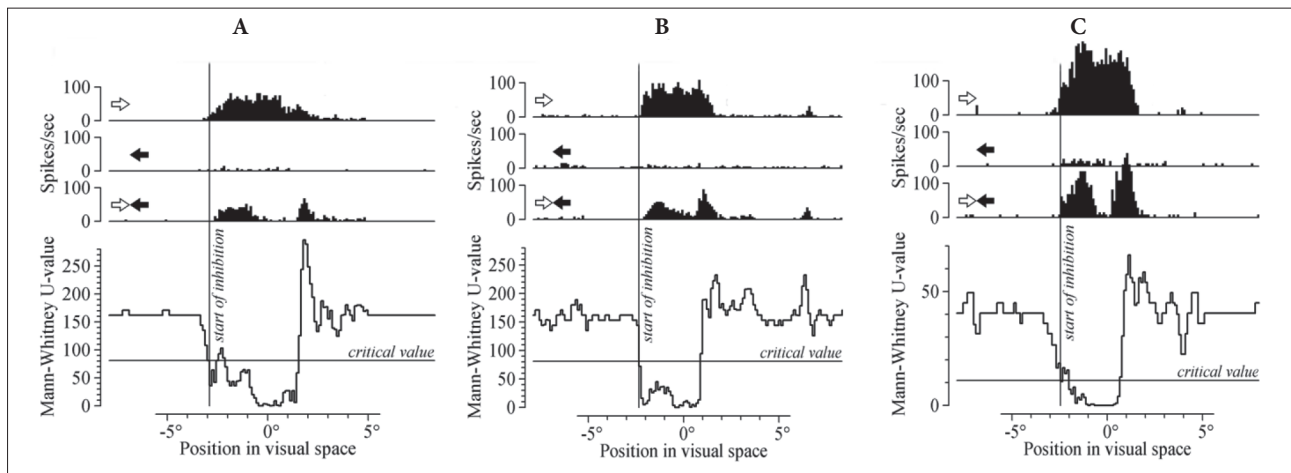


Fig. 9. Statistical analysis (Mann-Whitney test) of null-side inhibitory influences in three DS GCs of *Carassius gibelio* selective to different directions of stimulus movements. RFs of all DS units were located approximately in the center of the stimulation area. Mann-Whitney U-values presented on bottom panels were calculated at different positions of the preferred-side stripe in the stimulation area for two samples of data (single stripe moving in the preferred direction and paired stimuli moving in opposing directions). U-values were calculated over narrow intervals occupying 20' of the fish visual field. When the U-values fell below the critical level it was considered that the inhibitory effect from the null side was initiated at that point (position of the preferred side stripe at that moment is marked by the solid vertical line signed as “start of inhibition”; criterion U-value was fixed at $\alpha = 0.05$). **A** – ON-type DS GC selective to caudorostral movement. The unit was stimulated by 30' wide white stripes, that moved with a velocity of 5.5°/s along the horizontal axis of the fish visual field. Eighteen consecutive presentations of stimuli were performed at each step of stimulation. **B** – ON-type DS GC selective to ventrodorsal movement. The unit was stimulated by 30' wide white stripes that moved with a velocity of 5.5°/s along the vertical axis of the fish visual field. Eighteen consecutive presentations of stimuli were performed at each step of the stimulation. **C** – ON-type DS GC selective to dorsoventral movement. The unit was stimulated by 10' wide white stripes that moved with a velocity of 2.75°/s along the vertical axis of the fish visual field. Nine consecutive presentations of stimuli were performed at each step of the stimulation. Other conventions are same as in Fig. 8. Redesigned from [22].

over sufficiently small space intervals distributed along the motion trajectory of the preferred-side stimulus. If the responses to the two different stimuli matched, it was assumed that there was no inhibitory influence from the null side. But when the response to the paired stripes apparently decreased and the difference between the responses to the two types of stimuli (single and paired stripes) became statistically significant, it was assumed that the null-side inhibitory effect was initiated at that point. For the relevant statistical analysis, the nonparametric Mann-Whitney U-test was used. As mentioned above, in different experiments the stimulation was repeated either 9 or 18 times for each type of stimulus. Hence, we had to compare two equal samples with 9 or 18 sets of data over each small space interval. The length of this space interval was 20' of the visual field. The data obtained for such a small interval along the motion trajectory of the preferred-side stripe allowed us to determine the dependence of the Mann-Whitney U-values on the position of the preferred stimulus in the unit RF. The point at which the U-value fell below the critical level was considered as the beginning of inhibition. The

results of statistical analysis processed for three ON DS GCs of *Carassius gibelio* preferring caudorostral, ventrodorsal and dorsoventral directions of stimulus movement are presented in Fig. 9. In all demonstrated units, the influences of inhibitory signals were spread across the entire RF. Experiments with paired stripes were performed in three fish species, goldfish, carp and barbel. A total number of 52 DS GCs were subjected to this experimental procedure and in all a null-side inhibitory effect was observed. Inhibitory effects were spread across the entire RF in 62% of all DS GCs. In the remaining 38% units, inhibition was initiated inside the RF at different distances between the opposing stimuli. There are several notable spatial characteristics of the null-side inhibitory influences that were observed in the majority of the recorded DS GCs. In general, inhibitory signals induced at large distances between stimuli (early phase of inhibition) influenced the preferred-side response but did not occlude the response completely. In the late phase of inhibition when the stimuli moved closer to each other, the influence of the null-side stimulus significantly increased, and the response of the cell was completely

occluded. The onset of the late phase of inhibition was usually associated with the moment when the response to paired stimuli started to decline abruptly. After the stripes crossed each other in the center of the stimulation area, the response of the unit recovered.

Before discussing the results of our study [22], we would like to focus on one very important property of the DS circuitry described in the mammalian retina. Dendritic SACs innervating DS GCs were shown to overlap [34]. In their early work, Masland et al. [35] postulated that their excessive coverage was needed to create local subunits of the DS GC. Later it was suggested that the individual sectors of the starburst dendritic arbor act as independent local units and that these sectors are individually direction selective, creating a directional input to the DS GC [36]. The sectors are smaller than the dendritic field of targeted DS GC, thus accounting for the GC's ability to discriminate between subtle movements within the field. Such organization of DS circuitry provides DS GCs with a receptive field 500 μm in diameter to discriminate 40 μm movements anywhere within its receptive field [37]. As mentioned in the previous chapter, fish DS GCs that were studied in our experiments are characterized by similar properties [24]. The minimum resolvable angle for all tested DS GCs was close to the limit determined by the density of cones. To achieve such a high spatial resolution, it is necessary to compose the RF of many subunits with significantly smaller zones of signal summation. Recently, detailed statistical analyses of SAC-DS GC connectivity in the mouse retina using new electron microscopy techniques were performed [21]. They showed that the vast majority of SAC synapses are located at the GC's null side. It was also demonstrated that the SACs' dendritic arbors are composed of four independent (isolated) sectors. Each of them provides input to distinct DS GCs that prefer different directions of stimulus movement. Inputs to DS GCs are provided via dendrites aimed at the null direction of the corresponding DS unit. Hence, the results of the study argue that the null-side inhibitory mechanism of underlying direction selectivity is based on postsynaptic processing, i.e., on postsynaptic inhibition from SACs within a local dendritic region of DS GC. However, in a newer study [38], it was shown that mouse ON-OFF DS GCs receive both postsynaptic null-side inhibitory inputs from SACs and direction-tuned inputs from distinct types of bipolar cells. In

other words, besides the postsynaptic mechanism, evidence of an additional presynaptic inhibitory mechanism set up at bipolar cell terminals was provided for mammalian ON-OFF DS units.

Similar physiological properties in mammalian and fish DS GCs projecting to the tectum suggest that the direction selectivity in both types of units is most likely organized identically. Thus, the dynamics of null-side inhibitory influences during the opposing motion in fish DS GCs [22] may be discussed based on DS circuitry comprising both presynaptic and postsynaptic DS mechanisms [38]. We can offer the following hypothesis. During the early phase, counter-motion stimuli on the opposite sides of the DS GC receptive field act independently. While the preferred side of the DS GC dendritic tree is depolarized by the preferred-side stimulus, the opposite side of the RF is hyperpolarized due to postsynaptic inhibitory influences on the null side of the unit RF. Consequently, the response of GCs elicited by the preferred stripe was decreased but not occluded completely. At the late phase of inhibition when stripes move closer to each other, both stimuli act in almost the same region of the RF. In this case, abrupt decay and complete loss of the unit response may occur due to the influence of both presynaptic and postsynaptic inhibitory mechanisms activated by the null-side stripe. In other words, we cannot exclude the possible involvement of a presynaptic inhibitory mechanism in the late phase of opposing motion.

Segregation of retinal projections in the fish tectal retinorecipient layer

With the new setup, we managed to accurately determine the depth at which we could record different retinal GC projections in the tectal retinorecipient layer. Thirteen types of GCs projecting to the fish TO were described [1,16,23,39-42] (Fig. 10B). Their axon terminals are distributed in the following way: the responses of six types of DS GCs, which have been thoroughly described above, are regularly recorded in the superficial sublaminae at a depth of around 50 μm . The responses of several different types of units are regularly recorded in the second thick sublaminae approximately 50 μm deeper. Among them, the most numerous are responses of orientation-selective (OS) GCs. There are two types of OS units sensitive to either vertically or horizontally oriented edges or

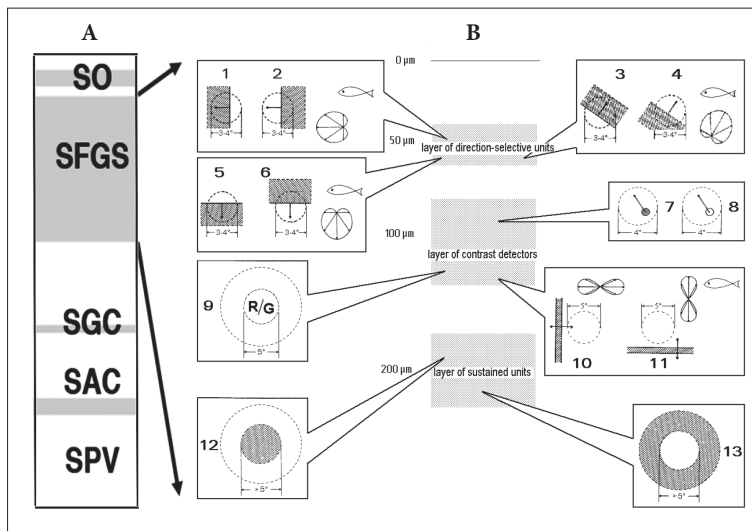


Fig. 10. Segregation of different types of retinal projections in the fish tectal retinorecipient layer (thickness of the retinorecipient layer is 200 μm). **A** – Schematic presentation of layers in the fish tectum opticum. SO – stratum opticum; SFGS – stratum fibrosum et griseum superficiale (retinorecipient layer); SGC – stratum griseum centrale; SAC – stratum album centrale; SPV – stratum periventriculare. **B** – Laminar organization of retinal projections in the tectal retinorecipient layer (SFGS). Superficial sublayer (at a depth of about 50 μm): 1 – ON DS caudorostral unit, responding when a dark edge moves out of its RF (circle area of 4–5°) in the caudorostral direction (indicated by an arrow); 2 – OFF caudorostral DS unit responding when a dark edge moves into the RF; in the bottom right corner of the frame is a polar diagram for the caudorostral units. In two other frames, the ON and OFF units of the ventrodorsal (3 and 4) and dorsoventral (5 and 6) preferred directions are presented. Other conventions are the same as in 1 and 2. Medial sublayer (at a depth of about 100 μm): detectors of black and white spots (7, 8), rarely recorded color-coding GCs (9), detectors of horizontal (11) and vertical (10) lines are shown. Adequate stimuli – vertical (10) and horizontal (11) stripes are presented near the corresponding eight-shape plots. The deepest sublayer (at a depth of about 200 μm): Two types of sustained units are shown – those activated by the darkening (12) and others activated by lightening (13) of their RFs. Redesigned from [42].

stripes (both are ON-OFF-type cells). The responses of other GCs, designated as spot detectors, are recorded at approximately the same depth in the TO. These units are divided into two subtypes of cells sensitive to small moving and stationary contrast spots that are brighter or darker than the background (ON and OFF units, respectively). In the same sublamina and a little deeper, the responses of another cell type are rarely encountered (color-opposing GCs of R/G type). Finally, the two types of sustained units that provide responses that increase to either darkening or lightening of their RFs are constantly recorded in the deepest sublaminae of the tectal retinorecipient layer (OFF- and ON-sustained units; depth of recording around 200 μm).

There are three methods that are currently used in studies of the fish retinotectal system. The first is classical microelectrode recording of the single responses from the GC terminals in the TO of an adult living specimen (used in our studies). Also, relatively new methods have been developed, such as Ca^{2+} imaging as well as genetic markers of certain neurons in transparent *Danio* larvae (in particular Brainbow genetic labeling). Each of these three methods has certain constraints and advantages, and when combined, they can provide a sufficiently meaningful representation of the organization of the retinotectal system. Fine lamination of GC axon terminals similar to that described in our studies has been demonstrated in the TO of zebrafish larvae by the Brainbow genetic technique [4,43–45]. These studies have revealed that the retinotectal projections of larval zebrafish are anatomically and functionally divided into fine sublaminae. It was demonstrated that lamination serves to spatially segregate inputs from retinal GC projections based on the type of information they transmit. The fact that this type of organization of the retinotectal projections appears as early as the larval developmental stage has also been shown by Ca^{2+} imaging [2,46].

Direction-selective neurons of the fish tectum: response pattern and classification

Besides the retinal DS GCs described above, other types of DS units presumably of tectal origin were recorded in the fish tectum. In an early study performed on different marine fishes [11], DS units were recorded beneath the sublaminae where the sustained units are located, i.e. beneath the retinorecipient layer. The amplitudes of spikes in the discharges of these units were much higher than those of the retinal elements (around 300 μV) and sometimes exceeded 1 mV. These putative tectal DS neurons were characterized by very large receptive fields (up to 60°), unlike the 4–5° of the units of retinal origin. Fig. 11A demonstrates a tectal

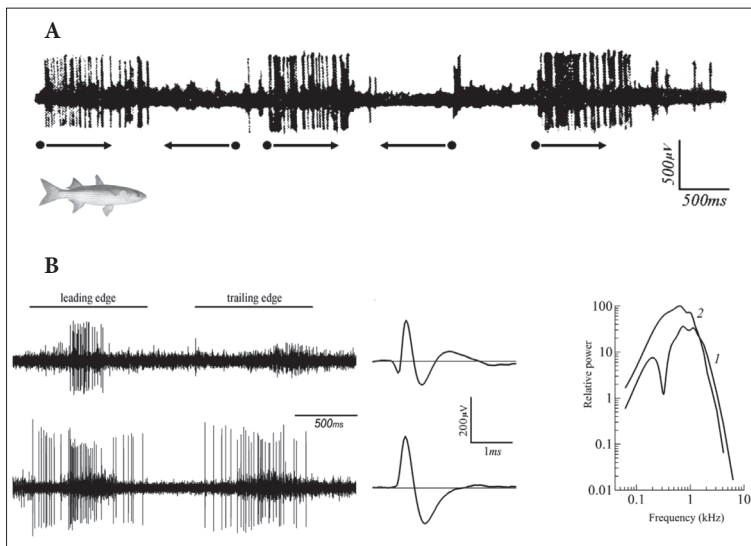


Fig. 11. Response pattern of direction selective neurons of the fish tectum. **A** – Responses of a tectal DS neuron of a mullet to stimuli moving in different directions. Stimuli (dark spots) moved in the caudorostral and opposite, rostrocaudal directions (arrows indicate the directions of the stimulus movement relative to fish orientation). One can see that the movement of spots in the caudorostral direction always evokes prominent spike discharge of the DS neuron, whereas the stimulus motion in the opposite direction does not induce a response of the unit. **B** – Responses of two goldfish DS units of different origin. Left panels: firing patterns of two DS units in response to the movement of leading and trailing edges of the broad stripe (“edge stimulus”). The first unit (upper trace) is a retinal OFF-type DS GC stimulated by the caudorostral movement of a broad black stripe on a neutral gray background with a speed of 11°/s; the second (lower trace) is a tectal DS neuron stimulated by downward movement of a broad white stripe on a black background with the same speed. Middle panels: averaged spike forms for retinal DS GC (upper trace; N=42), and tectal DS neuron (lower trace; N=61) shown in an expanded time scale. Right panel: power spectra for spikes of DS GC (1) and tectal DS neuron (2). Redesigned from [11,16].

DS neuron recorded in mullet, which preferred the caudorostral direction of movement.

These tectal DS units are characterized by fine spatial resolution and extremely high contrast sensitivity, similar to retinal DS GCs [47]. In more recent studies [16,48–49] it was shown that the responses of tectal neurons (TNs) with direction-selective properties can be recorded not only in deep tectal zones but also in the tectal retinorecipient layer, mainly in the sublaminae located underneath the zone of DS GC projections.

Several studies proposed the physiological criteria to classify units either as retinal or tectal [13,16,49–50]. The fact that DS units with the same properties as those described in the tectum have been recorded in fish retina [51–53] and the optic chiasma [8] favors

their retinal origin. However, a large RF, the pronounced spontaneous activity of a unit and the plasticity of its responses suggest its tectal origin [50]. The main differences in the responses of putative tectal and retinal DS units are illustrated in Fig. 11B. Two presented units were simultaneously recorded from the retinorecipient layer in the TO of a goldfish. The OFF-DS GC of presumably retinal origin preferred the caudorostral direction of the moving stimuli (Fig. 11B, left panel). It responded prominently to the leading edge of a black broad stripe moving across the neutral gray background within the RF and did not respond to the trailing edge of the stimulus. On the other hand, the putative tectal DS unit, which preferred the dorsoventral direction, responded to the moving edges of any sign of contrast (ON-OFF type of unit). This unit had a large RF based on the duration of the spike train. As for the features of spike trains recorded in the retinal and tectal DS units, the arriving spikes of DS GCs usually had approximately equal amplitude, whereas the amplitude of the spikes generated by the DS neurons decreased substantially as the spike rate increased (compare spike discharges of two units shown in Fig. 11B, left panel). The forms of the spikes in the

discharge also serve as discriminating criteria. Thus, in extracellular recordings, spikes arriving from the retina usually have a triphasic waveform with a negative deflection before the main positive wave, whereas spikes that are recorded in the vicinity of the cell body of tectal neurons are biphasic and lack such a deflection [13,16]. The difference in spike forms between two units is presented in the middle panel of Fig. 11B. We have also analyzed the power spectra of typical GC spikes and observed a drop in the spectrum of retinal DS units at a frequency close to 30 Hz. In this respect, they significantly differ from the power spectra of DS TNs (Fig. 11B, right panel). The validity of the above-mentioned criteria was proven experimentally [49]. In this study, we used cobalt, a universal blocker of synaptic transmission, as a crucial criterion to identify the

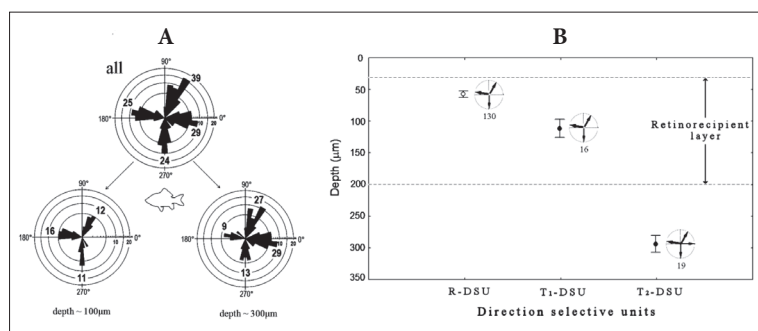


Fig. 12. Polar histograms of preferred directions for tectal DS neurons in fish. **A** – Histogram on the top (“all”): the distribution of preferred directions calculated in 117 tectal DS units (98 goldfish and 19 carp units). Lower histograms: the distribution of preferred directions for two groups of fish tectal DS units recorded at different tectal levels: at the tectal depth of about 100 μm (left histogram; 39 units) and at the tectal depth of about 300 μm (right panel; 78 units). **B** – Relative depth distribution of DS units in the fish tectum based on accurate measurements of tectal DS responses. Averaged depths in “ μm ” for all recorded units are shown. Open circle – retinal DS GC projections to the TO (R-DSU). Closed circles – tectal DS units: those recorded in the retinorecipient layer (T1-DSU) and others recorded in deep tectal zones (T2-DSU). Vertical bars denote 0.95 confidence intervals. Direction preferences of retinal and tectal DS units are given near the corresponding plotted data (the number of analyzed units is demonstrated). Retinal DS GCs proved to comprise three distinct types which prefer caudorostral, dorsoventral and ventrodorsal directions of stimulus movement. The fourth rostrocaudal preference emerges in a deep group of tectal DS units exclusively. Clear segregation of two groups of tectal DS units (T1-DSU and T2-DSU) was statistically proven (one-way ANOVA). The data were collected from 38 experiments conducted on 32 goldfish and 6 carps. Abscissa – various groups of DS units; ordinate – recording depths in “ μm ”. Redesigned from [48].

source of different responses recorded in the tectum. To block synaptic transmission, 50-100 μL of 100 mM CoCl_2 in Ringer’s solution was applied to the tectal surface and allowed to diffuse to the site of the recording. Responses of DS GCs and other retinal units (OS GCs, spot detectors, sustained units) were not affected by the application of cobalt. In contrast, units defined as DS TNs ceased firing, which indicated their tectal origin. After the cobalt solution was washed out with pure Ringer’s solution, the responses of the tectal DS units recovered.

A thorough classification of the tectal DS neurons according to their preferred direction was implemented recently. Recent data obtained in goldfish and carp unequivocally demonstrated that the responses of ON-OFF type tectal DS neurons can be recorded in TO at two different levels (Fig. 12A) [48-49]. The first cluster of tectal DS units was recorded much deeper in the TO, at a depth of about 300 μm , i.e. 100 μm deeper than the retinorecipient layer [41,48,54]. Four types of

DS TNs’ responses are regularly recorded in deep TO layers. In addition to the three types of DS TNs with preferred directions as those recorded for retinal DS GCs, a fourth type that preferred the rostrocaudal direction of movement (lacking in the retina) was regularly recorded [48,54]. The responses of the second cluster of tectal DS units are recorded more superficially in the retinorecipient layer, about 50 μm deeper than the sublayer of retinal DS GCs’ projections. Three types of DS TNs’ responses were recorded at this sublamina. Their preferred directions of motion are almost the same as those already identified for the units at the retinal level – caudorostral, ventrodorsal and dorsoventral. Thanks to modern equipment (e.g. the micromanipulator MP-225, Sutter Instrument), in the last few years we were able to perform more accurate measurements of the depth positions for various units recorded in the fish tectum. The data of these measurements collected in goldfish and carp from 38 experiments confirmed clear stratification of the two groups of tectal DS units (Fig.12B).

Direction-selective neurons of tectal origin were also identified in zebrafish larvae in several electrophysiological studies [55-57]. In a complex electrophysiological and morphological study [56], the structure and function of single DS TNs were compared by Ca^{2+} imaging and multiphoton-targeted patch-clamp recordings. The authors managed to identify two types of tectal DS neurons, preferring caudorostral and rostrocaudal directions. Both labeled types of neurons had their cell bodies in the deep periventricular layer, while their long afferents projected dorsally to the retinorecipient layer. In more detailed calcium imaging studies, two populations of tectal DS units in zebrafish larvae were identified [46,58]. Cell bodies of the major part of the recorded cells were in the deep, periventricular zone of the TO, while other DS units were identified in the tectal superficial layers located above the zone of DS GC projections in the stratum opticum. As in goldfish, zebrafish DS neurons have four preferred directions, three of them compatible with those already described for the retinal DS GCs. Like

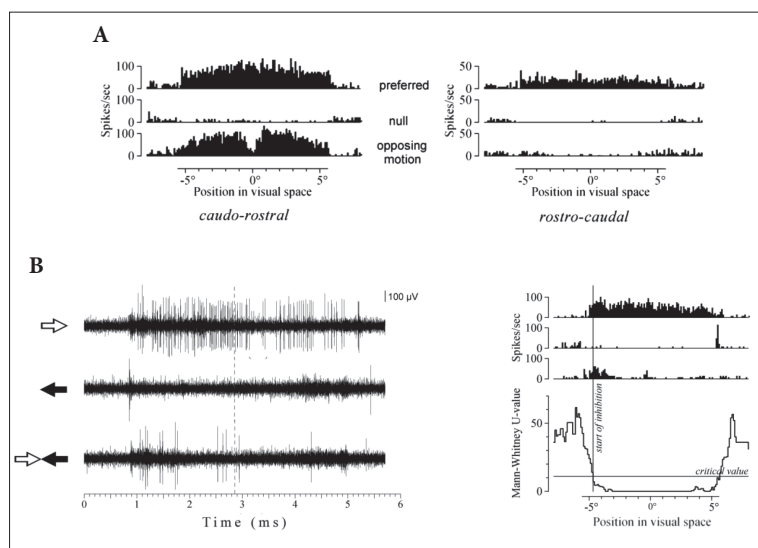


Fig. 13. Null-side inhibition in goldfish direction selective tectal neurons. **A** – Averaged peristimulus histograms calculated for all three modes of stimulation for 2 DS TNs, preferring caudo-rostral (left) and rostrocaudal (right) directions of stimulus movement, respectively. Nine consecutive presentations of stimuli were performed at each step of stimulation. The caudo-rostral unit was stimulated by 10° wide white stripes, rostrocaudal with 30° wide white stripes. Stimuli moved with a velocity of 2.75°/s along the horizontal axis of the fish visual field. Other conventions are same as in Fig. 8. **B** – Statistical analysis (Mann-Whitney test) of null-side inhibitory influences in another DS TN of *Carassius gibelio* selective to the rostrocaudal direction of motion. Left panel: spike discharges of the rostrocaudal DS TN evoked at three modes of stimulation. Vertical dashed line marks the moment at which counter stripes crossed each other in the center of the stimulation area. Right panel: Mann-Whitney U-values presented on lower panels were calculated at different positions of the preferred-side stripe in the stimulation area for two samples of data (single stripe moving in the preferred direction and paired stimuli moving in opposing directions). U-values were calculated over narrow intervals occupying 40° of the fish visual field. When the U-values fell below the critical level it was considered that the inhibitory effect from the null side was initiated at that point (position of the preferred side stripe at that moment is marked by the solid vertical line signed as “start of inhibition”; criterion U-value was fixed at the $\alpha=0.05$). The unit was stimulated by 30° wide white stripes that moved with the velocity of 2.75°/s along the horizontal axis of the fish visual field. Nine consecutive presentations of stimuli were performed at each step of the stimulation. Other conventions are same as in Fig. 8.

our findings, the authors identified the fourth population of DS tectal cells with the emergent rostrocaudal preference that was not present in any of the DS GC inputs. The fourth type of DS neurons was recorded only in the deep tectal layers, as in the case of goldfish.

In our studies, the DS responses of neuronal origin were recorded not only in the periventricular area but also in the retinorecipient layer in the zone slightly deeper than the DS retinal afferents. The direction of movement in the tectum of goldfish and carp is encoded both in the deep periventricular

zone and in the retinorecipient layer by three subtypes of DS TN responses tuned to the same directions of movement already identified at the retinal level [48]. Matching of three preferred directions of ON and OFF DS GCs and ON-OFF DS TNs allowed us to assume that the GCs with caudo-rostral, ventrodorsal and dorsoventral preferences are input neurons for the corresponding types of DS TNs. Based on morphological data on tectal DS neurons [56], we hypothesize that three types of DS responses in the deep TO zone can be recorded from the cell bodies of corresponding types of tectal DS neurons, while the more superficial DS responses, recorded in the retinorecipient layer, originate from the afferents of the same three types of DS TNs. On the other hand, the rostrocaudal preference in the fourth type of DS TNs recorded exclusively in the deep tectal zone is an emergent property of the TO. In our most recent experiments, we proved that direction selectivity in the “rostrocaudal” neurons is mediated by null-side inhibition. The experimental method described above was applied to DS TNs, with pairs of narrow stripes moving in opposing directions. In three types of DS TNs, which prefer the same directions as DS GCs, the inhibition mediated from the null side of the RF arose during the approach of stimuli and it ceased after the stripes crossed into the center of the stimulation area, similar to what was shown for retinal DS units (Fig. 13A, left panel). A significant-

ly different effect of null-side inhibition was observed in DS neurons of the fourth type, which prefer rostrocaudal movement. A pronounced inhibitory effect often manifested by the complete elimination of the response during opposing motion was recorded (Fig. 13B). The mechanism of null-side inhibition recorded in the RF of rostrocaudal TNs remains to be clarified.

The stratum opticum, the superficial layer of the TO, is composed of a population of GABAergic neurons, superficial inhibitory neurons (SINs) [59]. In studies conducted on zebrafish larvae [46,58] it was

demonstrated that at least part of the population of SINS is direction selective. Unlike periventricular DS TNs, the direction of motion in the superficial stratum opticum was encoded by three direction-selective subtypes of SINS tuned to upward, downward and caudal-to-rostral motion. We have also recorded from superficial neurons (presumably SINS) above the zone of the retinal DS projections [54]. However, these neurons did not express selectivity to the direction of motion.

CONCLUSIONS

Using microelectrode recordings from the fish tectum opticum, we accurately described the laminar organization of retinal GCs projections in the tectal retinorecipient layer. Thirteen types of GCs projecting to the fish TO and distributed in three sublaminae were described. In the superficial sublamina, at the depth of around 50 μm , the responses from DS GC projections are regularly recorded. Six distinct types of retinal DS units were determined. They can be divided into three distinct groups according to their preferred directions of stimulus movement: caudorostral, dorsoventral and ventrodorsal. Each of these groups is comprised of both ON and OFF units in equal proportions. The results of our experiments performed on several marine and cyprinid fish species indicated that the properties of their DS GCs were identical to the properties of retinal DS units of goldfish and carp. Our findings were additionally confirmed in a calcium imaging study of the retinal DS GCs innervating the tectum of zebrafish larvae [2]. Three subtypes of retinal DS units projecting to the zebrafish tectum characterized by a preference for directions similar to those described in our experiments were identified. Consequently, we hypothesize that the system of DS GCs comprising six physiologically distinct subtypes might be a universal retinal DS circuitry in teleost fish.

The properties of fish retinal DS GCs projecting to the tectum discussed in this review, namely the relatively small RF sizes and finest spatial resolution, characterize these units as local motion detectors similar to the fast DS GCs of the mammalian retina projecting to the superior colliculus. Direction selectivity in the fish DS GCs is mediated by asymmetric null-side inhibition, and in this respect these units also resemble the fast DS GCs of mammals. However,

it is important to note that our experiments revealed some essential differences between fish and mammalian fast DS GCs. Fish DS units are characterized by three preferred directions and use separate ON and OFF channels, while the mammalian DS GCs are represented by four types of ON-OFF cells with the preferred directions separated by about 90°. Nevertheless, the fourth rostrocaudal preferred direction is present in the fish visual system, though not at the level of the retinal DS cells but among the DS neurons of the fish tectum. Four types of ON-OFF DS neurons preferring different directions of motion were recorded. Their cell bodies are most likely located in the deep periventricular layer of the TO. The preferred directions of three types of DS TNs match the preferred directions of the three types of DS GCs. Matching of three preferred directions of ON and OFF DS GCs and ON-OFF DS TNs has allowed us to hypothesize that the GCs with caudorostral, ventrodorsal and dorsoventral preferences are input neurons for corresponding types of DS TNs. On the other hand, the rostrocaudal preference in the fourth type of DS TNs recorded exclusively in the deep tectal zone, is an emergent property of the TO. It was proven that the direction selectivity in these DS neurons is mediated by null-side inhibition generated at the tectal level. The underlying mechanism of the tectal asymmetric null-side inhibition remains to be clarified.

All the abovementioned facts emphasize the compatibility of the two DS mechanisms that exist in the retinotectal system of fish and in the retinocollicular system of mammals. It seems that in fish, as in other vertebrates, the retinotectal DS system is involved in detecting and tracking small objects moving in the surrounding environment.

Funding: Supported by the Russian Foundation for Basic Research, Grant No. 20-015-00063 A.

Acknowledgments: Research on the physiology of the fish visual system has been carried out in our laboratory for more than 50 years. We would like to dedicate this work to Dr. Vadim Maximov, the chief of our group during most of this period. He was the team leader whose scientific drive as well as meticulous experiment planning and data analysis supported all research findings.

Author contributions: All authors have contributed to the writing and revision of the manuscript.

Conflict of interest disclosure: The authors declare that there are no conflicts of interest relevant to this study.

REFERENCES

1. Maximov VV, Maximova EM, Maximov PV. Direction selectivity in the goldfish tectum revisited. *Ann NY Acad Sci.* 2005;1048:198-205. <https://doi.org/10.1196/annals.1342.018>
2. Nikolaou N, Lowe AS, Walker AS, Abbas F, Hunter PR, Thompson ID, Meyer MP. Parametric functional maps of visual inputs to the tectum. *Neuron.* 2012;76:317-24. <https://doi.org/10.1016/j.neuron.2012.08.040>
3. Northmore DPM. The optic tectum. In: Farrell AP, editor. *Encyclopedia of fish physiology: from genome to environment.* London: Elsevier; 2011. p 131-42. <https://doi.org/10.1111/j.1095-8649.2012.03269.x>
4. Robles E, Laurell E, Baier H. The retinal projectome reveals brain-area-specific visual representations generated by ganglion cell diversity. *Curr Biol.* 2014;24:2085-96. <https://doi.org/10.1016/j.cub.2014.07.080>
5. Lettvin JY, Maturana HR, McCulloch WS, Pitts, WH. What the frog's eye tells the frog's brain. *Proc Inst Radiol Eng NY.* 1959; 47:1940-51. <https://doi.org/10.1109/JRPROC.1959.287207>
6. Maturana HR, Lettvin JY, McCulloch WS, Pitts WH. Anatomy and physiology of vision in the frog. *J Gen Physiol.* 1960;43:129-75 <https://doi.org/10.1085/jgp.43.6.129>
7. Gesteland RC, Howland B, Lettvin JY, Pitts WH. Comments on microelectrodes. *Proc Inst Radio. Eng NY.* 1959;47:1856-62. <https://doi.org/10.1109/JRPROC.1959.287156>
8. Jacobson M, Gaze RM. Types of visual response from single units in the optic tectum and optic nerve of the goldfish. *Q J Exp Physiol.* 1964;49:199-209. <https://doi.org/10.1113/expphysiol.1964.sp001720>
9. Cronly-Dillon JR. Units sensitive to direction of movement in goldfish tectum. *Nature.* 1964;203:214-5. <https://doi.org/10.1038/203214a0>
10. Liege B, Galand G. Types of single-unit visual responses in the trout's optic tectum. In: Gudikov A editor. *Visual Information Processing and Control of Motor Activity.* Sofia: Bulgarian Academy of Sciences; 1971. p. 63-5.
11. Maximova EM, Orlov OYu, Dimentman AM. Investigation of visual system of some marine fishes. *Voproc Ichtiologii.* 1971; 11:893-9. Russian.
12. Maximova EM, Dimentman AM, Maximov VV, Nikolayev PP, Orlov OY. The physiological mechanisms of colour constancy. *Neirofiziologiya.* 1975;7:21-6. Russian. <https://doi.org/10.1007/BF01063019>
13. Wartzok D, Marks WB. Directionally selective visual units recorded in optic tectum of the goldfish. *J Neurophysiol.* 1973;36:588-604. <https://doi.org/10.1152/jn.1973.36.4.588>
14. Zenkin GM, Pigarev IN. Detector properties of the ganglion cells of the pike retina. *Biofizika.* 1969;14:722-30. Russian.
15. Maximova EM, Maximov VV. Detectors of the oriented lines in the visual system of the fish *Carassius carassius.* *J Evol Biochem Phys.* 1981;17:519-25. Russian.
16. Maximov VV, Maximova EM, Maximov PV. Classification of direction-selective units recorded in the goldfish tectum. *Sensornye Sistemy.* 2005b;19:322-35. Russian.
17. Barlow HB, Levick WR. The mechanism of directionally selective units in rabbit's retina. *J Physiol.* 1965;178:477-504. <https://doi.org/10.1113/jphysiol.1965.sp007638>
18. Borst A, Euler T. Seeing things in motion: models, circuits, and mechanisms. *Neuron.* 2011;71:974-94. <https://doi.org/10.1016/j.neuron.2011.08.031>
19. Vaney DI, Sivyer DI, Taylor WR. Direction selectivity in the retina: symmetry and asymmetry in structure and function. *Nat Rev Neurosci.* 2012;13:194-208. <https://doi.org/10.1038/nrn3165>
20. Oyster CW, Barlow HB. Direction-selective units in rabbit retina: Distribution of preferred directions. *Science.* 1967; 155:841-2. <https://doi.org/10.1126/science.155.3764.841>
21. Briggman KL, Helmstaedter M, Denk W. Wiring specificity in the direction-selectivity circuit of the retina. *Nature.* 2011;471:183-8. <https://doi.org/10.1038/nature09818>
22. Damjanović I, Maximova EM, Aliper AT, Maximov PV, Maximov VV. Opposing motion inhibits responses of direction-selective ganglion cells in the fish retina. *J Integr Neurosci.* 2015;14:53-72. <https://doi.org/10.1142/S0219635215500077>
23. Damjanović I, Maximova EM, Maximov VV. Receptive field sizes of direction-selective units in the fish tectum. *J Integr Neurosci.* 2009;8:77-93. <https://doi.org/10.1142/S021963520900206X>
24. Maximov VV, Maximova EM, Damjanović I, Maximov PV. Detection and resolution of drifting gratings by motion detectors in the fish retina. *J Integr Neurosci.* 2013;12:117-43. <https://doi.org/10.1142/S0219635213500015>
25. Maximova EM, Govardovskii VI, Maximov PV, Maximov VV. Spectral sensitivity of direction-selective ganglion cells in the fish retina. *Ann NY Acad Sci.* 2005;1048:433-4.
26. Maximova EM, Levichkina EV, Utina IA. Morphology of putative direction-selective ganglion cells traced with Dii in the fish retina. *Sensornye Sistemy.* 2006;20:279-87. Russian.
27. Oyster CW, Takahashi E, Collewijn H. Direction-selective retinal ganglion cells and control of optokinetic nystagmus in the rabbit. *Vision Res.* 1972; 12:183-93. [https://doi.org/10.1016/0042-6989\(72\)90110-1](https://doi.org/10.1016/0042-6989(72)90110-1)
28. Wyatt HJ, Daw NW. Directionally sensitive ganglion cells in the rabbit retina: Specificity for stimulus direction, size, and speed. *J Neurophysiol.* 1975;38:613-26. <https://doi.org/10.1152/jn.1975.38.3.613>
29. Grzywacz NM, Amthor FR. Robust directional computation in on-off irectionally selective ganglion cells of rabbit retina. *Vis Neurosci.* 2007;24:647-61. <https://doi.org/10.1017/S0952523807070666>
30. Lee S, Kim K, Zhou ZJ. Role of ACh-GABA cotransmission in detecting image motion and motion direction. *Neuron.* 2010;68:1159-72. <https://doi.org/10.1016/j.neuron.2010.11.031>
31. Brandon C. Cholinergic amacrine neurons of the dogfish retina. *Vis Neurosci.* 1991;6:553-62. <https://doi.org/10.1017/s0952523800002534>
32. Yazulla S, Studholme KM. Neurochemical anatomy of the zebrafish retina as determined by immunocytochemistry. *J Neurocyt.* 2001;30:551-92. <https://doi.org/10.1023/A:1016512617484>

33. Arenzana FJ, Clemente D, Sánchez-González, R, Porteros A, Aijón J, Arévalo, R. Development of the cholinergic system in the brain and retina of the zebrafish. *Brain Res Bull.* 2005;66:421-5. <https://doi.org/10.1016/j.brainresbull.2005.03.006>
34. Tauchi M, Masland RH. The shape and arrangement of the cholinergic neurons in the rabbit retina. *Proc R Soc Lond B Biol Sci.* 1984;223:101-19. <http://doi.org/10.1098/rspb.1984.0085>
35. Masland RH, Mills JW, Hayden SA. Acetylcholine-synthesizing amacrine cells: Identification and selective staining by using radioautography and fluorescent markers. *Proc R Soc Lond B Biol Sci.* 1984;223:79-100. <https://doi.org/10.1098/rspb.1984.0084>
36. Vaney DI, Young HM. GABA-like immunoreactivity in cholinergic amacrine cells of the rabbit retina. *Brain Res.* 1988;438:369-73. [https://doi.org/10.1016/0006-8993\(88\)91366-2](https://doi.org/10.1016/0006-8993(88)91366-2)
37. Masland RH. The neuronal organization of the retina. *Neuron.* 2012;76:266-80. <https://doi.org/10.1016/j.neuron.2012.10.002>
38. Matsumoto A, Agbariah W, Solveig Nolte S, Andrawos R, Levi H, Sabbah S, Yonehara K. Direction selectivity in retinal bipolar cell axon terminals. *Neuron.* 2021;109:1-15. <https://doi.org/10.1016/j.neuron.2021.11.004>
39. Maximov VV, Maximova EM, Maximov PV. Classification of orientation-selective units recorded in the goldfish tectum. *Sensornye Sistemy.* 2009;23:13-23. Russian.
40. Damjanović I, Maximova EM, Maximov VV. On the organization of receptive fields of orientation-selective units recorded in the fish tectum. *J Integr Neurosci.* 2009;8:323-44. <https://doi.org/10.1142/S0219635209002174>
41. Aliper AT, Zaichikova AA, Damjanović I, Maximov PV, Kasparson AA, Gačić Z, Maximova EM. Updated functional segregation of retinal ganglion cell projections in the tectum of a cyprinid fish. Further elaboration based on microelectrode recordings. *Fish Physiol Biochem.* 2019;45:773-92. <https://doi.org/10.1007/s10695-018-0603-0>
42. Maximova EM, Aliper AT, Damjanović I, Zaichikova AA, Maximov PV. On the organization of receptive fields of retinal spot detectors projecting to the fish tectum: Analogies with the local edge detectors in frogs and mammals. *J Comp Neurol.* 2020;528:1423-35. <https://doi.org/10.1002/cne.24824>
43. Nevin LM, Robles E, Baier H, Scot EK. Focusing on optic tectum circuitry through the lens of genetics. *BMC Biol.* 2010;8:126. <https://doi.org/10.1186/1741-7007-8-126>
44. Robles E, Smith SJ, Baier H. Characterization of genetically targeted neuron types in the zebrafish optic tectum. *Front Neural Circuit.* 2011;5:1. <https://doi.org/10.3389/fncir.2011.00001>
45. Robles E, Filosa A, Baier H. Precise lamination of retinal axons generates multiple parallel input pathways in the tectum. *J Neurosci.* 2013; 33:5027-39. <https://doi.org/10.1523/JNEUROSCI.4990-12.2013>
46. Abbas F, Triplett MA, Goodhill GJ, Meyer MP. 2017. A three-layer network model of direction selective circuits in the optic tectum. *Front Neural Circuits.* 2017;11:88. <https://doi.org/10.3389/fncir.2017.00088>
47. Damjanović I. Direction selective units in goldfish retina and tectum opticum - review and new aspects. *J Integr Neurosci.* 2015;14:535-556. <https://doi.org/10.1142/S0219635215300024>
48. Damjanović I, Maximov PV, Aliper AT, Zaichikova AA, Gačić Z, Maximova EM. Putative targets of direction-selective retinal ganglion cells in the tectum opticum of cyprinid fish. *Brain Res.* 2019;1708:20-6. <https://doi.org/10.1016/j.brainres.2018.12.006>
49. Maximova EM, Pushchin II, Maximov PV, Maximov VV. Presynaptic and postsynaptic single-unit responses in the goldfish tectum as revealed by a reversible synaptic transmission blocker. *J Integr Neurosci.* 2012;11:183-91. <https://doi.org/10.1142/S0219635212500136>
50. O'Benar JD. Electrophysiology of neural units in goldfish optic tectum. *Brain Res Bull.* 1976;1:529-41. [https://doi.org/10.1016/0361-9230\(76\)90080-0](https://doi.org/10.1016/0361-9230(76)90080-0)
51. Daw NW. Color coded units in the goldfish retina (PhD thesis). Baltimore: The Johns Hopkins University; 1967.
52. Bilotta J, Abramov I. Orientation and direction tuning of goldfish ganglion cells. *Visual Neurosci.* 1989;2:3-13. <https://doi.org/10.1017/s0952523800004260>
53. Tsvilling V, Donchin O, Shamir M, Segev R. Archer fish fast hunting maneuver may be guided by directionally selective retinal ganglion cells. *Eur J Neurosci.* 2012;35:436-44. <https://doi.org/10.1111/j.1460-9568.2011.07971.x>
54. Zaichikova A, Damjanović I, Maximov P, Aliper A, Maximova E. Neurons in the optic tectum of fish: Electrical activity and selection of appropriate stimulation. *Neurosci Behav Physiol.* 2021;51:993-1001. <https://doi.org/10.1007/s11055-021-01157-4>
55. Grama A, Engert F. Direction selectivity in the larval zebrafish tectum is mediated by asymmetric inhibition. *Front Neural Circuit.* 2012;6:59. <https://doi.org/10.3389/fncir.2012.00059>
56. Gabriel JP, Triverdi CA, Maurer CM, Ryu C, Bollman JH. Layer-specific targeting of direction-selective neurons in the zebrafish tectum opticum. *Neuron.* 2012;76:1147-60. <https://doi.org/10.1016/j.neuron.2012.12.003>
57. Gebhardt C, Baier H, Del Bene F. Direction selectivity in the visual system of the zebrafish arva. *Front. Neural Circuit.* 2013;7:111. <https://doi.org/10.3389/fncir.2013.00111>
58. Hunter PR, Lowe AS, Thompson I, Meyer MP. Emergent properties of the optic tectum revealed by population analysis of direction and orientation selectivity. *J Neurosci.* 2013;33:13940-5. <https://doi.org/10.1523/JNEUROSCI.1493-13.2013>
59. Barker AJ, Baier H. SINS and SOMs: neural microcircuits for size tuning in the zebrafish and mouse visual pathway. *Front Neural Circuit.* 2013;7:89. <https://doi.org/10.3389/fncir.2013.00089>